



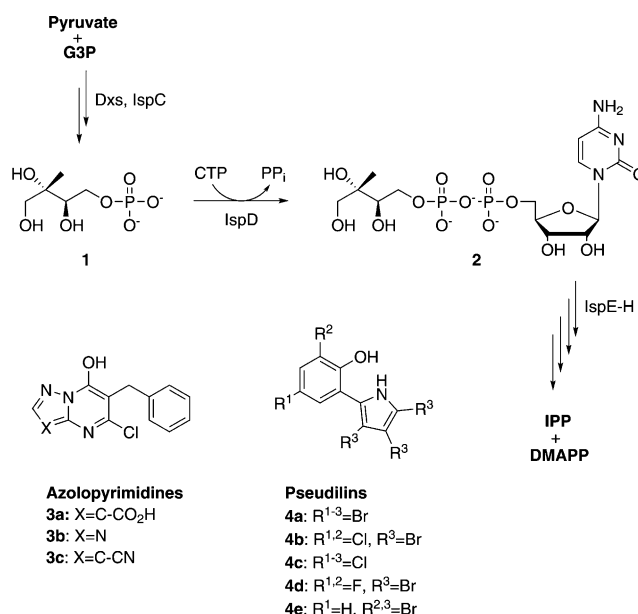
# Pseudilins: Halogenated, Allosteric Inhibitors of the Non-Mevalonate Pathway Enzyme IspD\*\*

Andrea Kunfermann, Matthias Witschel, Boris Illarionov, René Martin, Matthias Rottmann, H. Wolfgang Höffken, Michael Seet, Wolfgang Eisenreich, Hans-Joachim Knölker, Markus Fischer, Adelbert Bacher, Michael Groll, and François Diederich\*

**Abstract:** The enzymes of the non-mevalonate pathway for isoprenoid biosynthesis have been identified as attractive targets with novel modes of action for the development of herbicides for crop protection and agents against infectious diseases. This pathway is present in many pathogenic organisms and plants, but absent in mammals. By using high-throughput screening, we identified highly halogenated marine natural products, the pseudilins, to be inhibitors of the third enzyme, IspD, in the pathway. Their activity against the IspD enzymes from *Arabidopsis thaliana* and *Plasmodium vivax* was determined in photometric and NMR-based assays. Cocystal structures revealed that pseudilins bind to an allosteric pocket by using both divalent metal ion coordination and halogen bonding. The allosteric mode of action for preventing cosubstrate (CTP) binding at the active site was elucidated. Pseudilins show herbicidal activity in plant assays and antiparasmodial activity in cell-based assays.

Two of the most urgent challenges for humanity are the fight against nutritional problems and against infectious diseases, such as malaria<sup>[1]</sup> and tuberculosis.<sup>[2]</sup> Unfortunately, the key tools against those plagues (herbicides, which are essential for crop yields, and anti-infectives) suffer from rapid loss of efficacy because of increasing resistance of the targeted organisms. In an effort to cross-fertilize both fields, lead compounds from agrochemistry research have been examined against infectious germs.<sup>[3]</sup> Whereas animals exclusively use the mevalonate pathway for the biosynthesis of the terpenoid precursors isopentenyl diphosphate (IPP) and dimethylallyl diphosphate (DMAPP),<sup>[4]</sup> plants and many human pathogens utilize the non-mevalonate (also designated deoxyxylulose

phosphate (DXP)) pathway, which was discovered in the 1990s.<sup>[5]</sup> The seven enzymes of the non-mevalonate pathway (Scheme 1) are recognized drug targets.<sup>[6]</sup> Recent efforts in herbicide research have also demonstrated the importance of



**Scheme 1.** IspD-catalyzed reaction with the target compounds **3a–c** and **4a–e**. Ligands **4a–e** are shown in the *syn* conformation. G3P, glyceraldehyde-3-phosphate; **1**, 2C-methyl-D-erythritol-4-phosphate (MEP); **2**, 4-diphosphocytidyl-2C-methyl-D-erythritol (CDP-ME); IPP, isopentenyl diphosphate; DMAPP, dimethylallyl diphosphate.

[\*] Dr. M. Seet, Prof. Dr. F. Diederich  
Laboratorium für Organische Chemie, ETH Zürich  
Vladimir-Prelog-Weg 3, HCI, 8093 Zürich (Switzerland)  
E-mail: diederich@org.chem.ethz.ch

A. Kunfermann,<sup>[†]</sup> Prof. Dr. W. Eisenreich, Prof. Dr. M. Groll  
Center for Integrated Protein Science Munich  
Lehrstuhl für Biochemie, Technische Universität München  
Lichtenbergstrasse 4, 85748 Garching (Germany)

Dr. M. Witschel,<sup>[†]</sup> Dr. H. W. Höffken  
BASF SE  
Carl-Bosch-Strasse 38, 67056 Ludwigshafen (Germany)

Dr. B. Illarionov, Prof. Dr. M. Fischer, Prof. Dr. A. Bacher  
Hamburg School of Food Science, Universität Hamburg  
Grindelallee 117, 20146 Hamburg (Germany)

Dr. R. Martin, Prof. Dr. H.-J. Knölker  
Department Chemie, Technische Universität Dresden  
Bergstrasse 66, 01069 Dresden (Germany)

Dr. M. Rottmann  
Swiss Tropical and Public Health Institute (STPHI)  
Socinstrasse 57, 4051 Basel (Switzerland)  
and  
Universität Basel  
Petersplatz 1, 4003 Basel (Switzerland)

[†] These authors contributed equally to this work.

[\*\*] Pseudilins **4a**, **4b**, and **4e** were originally supplied to BASF SE, Ludwigshafen (Germany), by Prof. H. Laatsch.<sup>[14a,c]</sup> F. Röhl (BASF SE) conducted the high-throughput screening against AtIspD. C. Freymont (STPHI, Basel, Switzerland) performed the cell-based assays against *P. falciparum*. We thank the staff of the beamline X06SA at the Paul Scherrer Institute, Swiss Light Source, Villigen (Switzerland), for their help with data collection. Support by the ETH Research Council is acknowledged.



Supporting information for this article is available on the WWW under <http://dx.doi.org/10.1002/anie.201309557>.

this pathway.<sup>[7]</sup> The commercial herbicide ketoclozomazone inhibits Dxs, the first enzyme of the non-mevalonate pathway (for abbreviations see Scheme 1 and Figure S1 in the Supporting Information),<sup>[8]</sup> while the natural product fosmidomycin (which blocks IspC) has been evaluated in clinical trials against malaria.<sup>[9]</sup> The third enzyme of the pathway, IspD, converts 2C-methyl-D-erythritol 4-phosphate (MEP, **1**) into 4-diphosphocytidyl-2C-methyl-D-erythritol (CDP-ME, **2**), and we recently showed that synthetic azolopyrimidine derivatives **3a–c** (Scheme 1) inhibit IspD from *A. thaliana* (AtIspD) with IC<sub>50</sub> values in the low nanomolar range, thus indicating IspD is a potential target for drug development.<sup>[10]</sup>

Here, we report on the mode of action of pseudilin derivatives (Scheme 1), highly halogenated marine alkaloids<sup>[11]</sup> with herbicidal and antimalarial activity, against IspD. We determined the inhibitory potency in photometric and NMR-based activity assays by published procedures.<sup>[12]</sup> Moreover, these derivatives were analyzed in vitro for their efficacy against *Plasmodium falciparum*. The herbicidal activity of the pseudilins has already been described.<sup>[3]</sup> Here their allosteric binding properties were elucidated at the atomic level by crystallography of AtIspD complex structures, showing effective protein–ligand halogen bonding interactions.

To discover new chemical entities as herbicidal drug leads against IspD, a library containing about 100 000 compounds with druglike properties was screened by using a photometrically monitored assay.<sup>[12,13]</sup> This approach allowed us to identify hits with IC<sub>50</sub> values in the low micromolar range (<25 μM) against AtIspD (Table 1), namely compounds **4a** and **4b**, which belong to the class of pseudilins that were isolated in the 1960s from the marine bacterium *Pseudomonas bromoutilis*.<sup>[11a,14]</sup> The chemical scaffold of the screening hits differs significantly from that of the previously published synthetic azolopyrimidines, thereby suggesting that pseudilin derivatives might exhibit a new mode of action toward IspD.

To further investigate the pseudilin-type inhibitors, we synthesized **4a–e** by published procedures.<sup>[14,15]</sup> We started kinetic studies with the coupled assay by using three supplementary enzymes and three cosubstrates to enable a photometric readout of the reaction velocity (Table 1). The

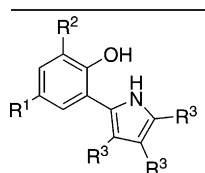
IC<sub>50</sub> values for the auxiliary enzymes are summarized in Table 1SI. Under assay conditions with 5 mM MgCl<sub>2</sub> but no other divalent cations, **4a** had an apparent IC<sub>50</sub> value of 13 μM. As elucidated by the crystal structures described below, cadmium(II) is in a chelate complex with the pseudilin derivatives. Therefore, CdSO<sub>4</sub> was added to the assay buffer to concentrations in the double-digit micromolar range, which was accompanied by a more than sevenfold increase in the inhibition. Similar effects were noted with compounds **4b** and **4c**. In comparison to the other derivatives, **4e** exhibits a decreased inhibition profile in the photometric assay, which is in agreement with the structural results. As shown for compound **4b** (Table 2SI), the binding preference could also be increased twofold by addition of other divalent cations (Ca<sup>2+</sup>, Cu<sup>2+</sup>, or Zn<sup>2+</sup>) in a concentration of 20 μM. We confirmed the photometrically monitored assay by quantitative <sup>31</sup>P NMR spectroscopy, which records simultaneously the concentrations of the IspD substrate **1** as well as the products **2** and diphosphate. These experiments revealed that the equilibrium for the IspD-catalyzed reaction is not predominantly on the product side. Therefore, the overall free energy gradient of the catalyzed reaction was increased by the addition of inorganic diphosphatase to convert the reaction product diphosphate into orthophosphate (see the Supporting Information for details of the assay). The IC<sub>50</sub> values determined by the two distinct methods agreed within a factor of 3 (IC<sub>50</sub> values are 1.4 ± 0.3 μM for compound **4a** and 7.5 ± 0.3 μM for compound **4e**), thus confirming that divalent metal ions are crucial components for the strong inhibition of IspD by pseudilin derivatives, except **4e**.

We also tested the pseudilin-type inhibitors against the blood stages of *P. falciparum*, the causative agent of malaria tropica, whose survival is dependent on the activity of the non-mevalonate pathway (Table 1).<sup>[16]</sup> The EC<sub>50</sub> values in the cell-based assay were in the 1–12 μM range, which suggests that IspD is the molecular target causing the antiparasitic activity of pseudilins. The cytotoxicity of **4a** against mammalian (rat) cells was found to be 3.1 μM. Hence, IspD of *P. vivax* (PvIspD)<sup>[17]</sup> was tested in a photometric activity assay against the identified candidates. Compared to AtIspD, a weaker inhibition in the double-digit micromolar range was detected

for the pseudilin derivatives studied in PvIspD. This, and the cytotoxicity seen in mammalian cells,<sup>[14c]</sup> indicates that the inhibition of the *P. falciparum* blood stages by the pseudilin-type inhibitors most probably involves molecular targets in addition to IspD. We thus next investigated the inhibition mechanisms at the atomic level of pseudilin derivatives causing the differences in the IspD binding among species.

We started the crystallographic study with the determination of the AtIspD apo structure at 1.5 Å resolution (PDB code: 4NAI). Details on the structure elucidation are

**Table 1:** IC<sub>50</sub> values of compounds **4a–e**, measured in the photometric assay against AtIspD and PvIspD with different concentrations of metal ions, and cell-based EC<sub>50</sub> values against *P. falciparum*.

ligand				IC <sub>50</sub> AtIspD <sup>[a]</sup> [μM]		IC <sub>50</sub> PvIspD <sup>[a]</sup> [μM]		EC <sub>50</sub> <i>Pf</i> cell <sup>[c]</sup> [μM]
	R <sup>1</sup>	R <sup>2</sup>	R <sup>3</sup>	without metal	40 μM Cd <sup>2+</sup>	without metal	40 μM Cd <sup>2+</sup>	
<b>4a</b>	Br	Br	Br	13 ± 2	1.4 ± 0.2	48 ± 9	57 ± 12	1.27
<b>4b</b>	Cl	Cl	Br	12 ± 1	2.2 ± 0.2	56 ± 8	41 ± 7	1.07
<b>4c</b>	Cl	Cl	Cl	19 ± 2	4.3 ± 0.8	46 ± 6	40 ± 7	n.d.
<b>4d</b>	F	F	Br	79 ± 6	13 ± 2	64 ± 15	51 ± 15	n.d.
<b>4e</b>	H	Br	Br	52 ± 6	19 ± 2	36 ± 10	24 ± 6	11.72

[a] Data sets have been treated with the program Dynafit to calculate the IC<sub>50</sub> values.<sup>[25]</sup> Values are the mean of three IC<sub>50</sub> values obtained from independent measurements. [b] In vitro activity on the *P. falciparum* NF54 strain. Values are the mean of three independent experiments. n.d., not determined.

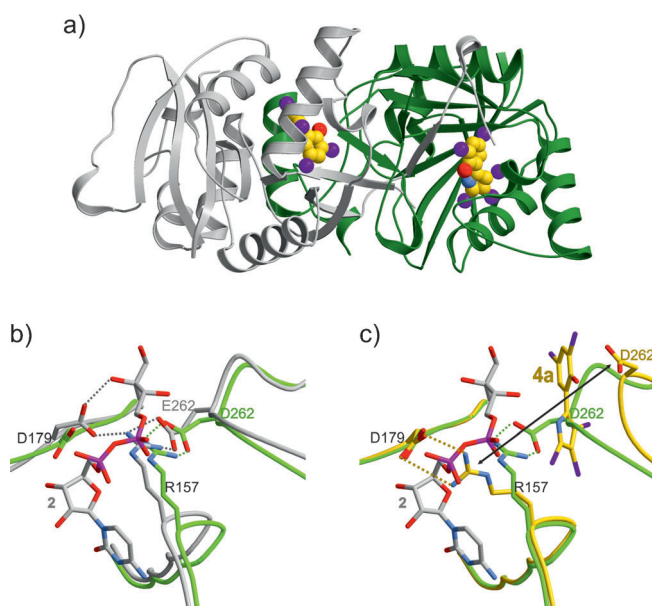


**Figure 1.** a) Overall structure of the AtIspD dimer in complex with compound **4a** shown as secondary structure elements. **4a** is presented as a ball and stick model. b) Structural superposition of the apo AtIspD structure (green) with the EcIspD:2 complex (gray; PDB code: 1INI).<sup>[18]</sup> Interactions are indicated by dashed lines. Conserved amino acids are shown in black (AtIspD numbering), whereas the remaining residues are shown according to the color of the respective enzyme. c) Structural superposition of apo AtIspD (green) with the AtIspD:4a complex (gold). Additionally, **2** from PDB code: 1INI is presented in gray. Stereoviews of (b) and (c) are shown in Figure 3SI.

provided in the Supporting Information and Table 3SI. AtIspD is physiologically present as a homodimer, and the subunit interface is mainly assembled over a linker region that points out of each monomer (Figure 1a). Notably, oligomerization is important for the binding of the cosubstrate (CTP) and thus, for enzyme activity. A comparison of the overall structures of AtIspD apo and IspD from *Escherichia coli* (EcIspD) in complex with the reaction product **2** (PDB code: 1INI)<sup>[18]</sup> revealed that the residues involved in dimer formation as well as amino acids that coordinate the diphosphate moiety of CTP are conserved among species (Figures 1b, 2SI, and 3SI). For clarity, only the AtIspD numbering is used to describe the amino acid residues here. At the active site of EcIspD, Asp179 interacts with and stabilizes both substrate **1** and product **2**. The binding of **1** and CTP is facilitated by only minor structural rearrangements, as depicted in the superposition (Figure 1b). Remarkably, the comparison of EcIspD and AtIspD revealed that Arg157 and Asp262, both hydrogen bonded near the active site, match perfectly, although Asp262 is a glutamate in the case of EcIspD. However, there is a major difference between the prokaryotic and eukaryotic IspD homologues: in the *E. coli* structure, Arg157 interacts with both Asp179 and Glu262, thereby stabilizing the active site cavity to facilitate substrate binding and turnover, whereas in AtIspD, Asp179 differs in its orientation, thus indicating that this position is species-specific.

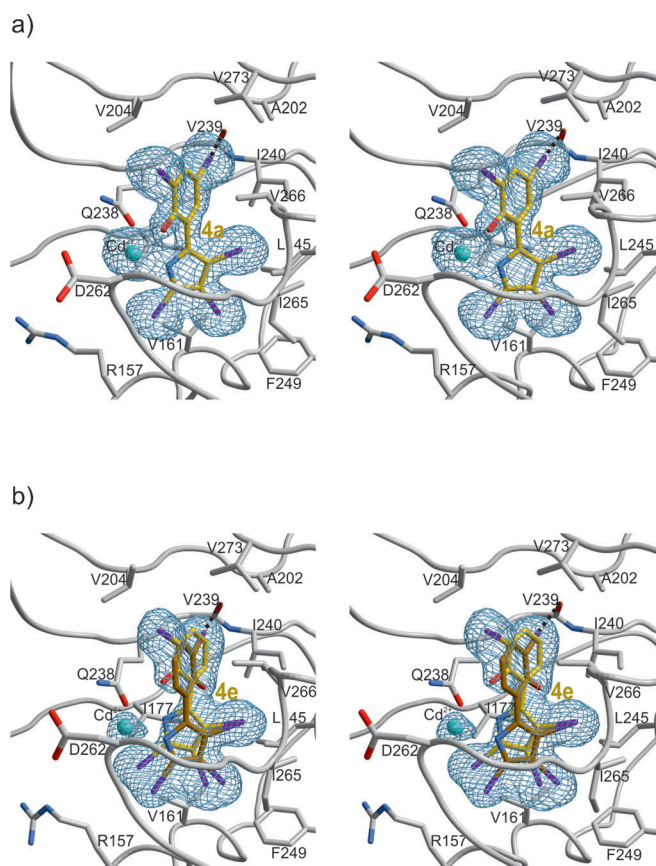


**Figure 2.** Stereoview of the allosteric site of AtIspD in complex with a) compound **4a** (PDB code: 4NAK) and b) compound **4e** (PDB code: 4NAN). **4e** is populated 7:3 as the *syn/anti* conformation. The  $2F_o - F_c$  electron density map (blue mesh) is contoured at 1.0  $\sigma$ . The ligand has been excluded prior to phase calculation to avoid any model bias. The allosteric site residues and the ligands **4a** and **4e** (gold) are presented as stick models,  $\text{Cd}^{2+}$  (cyan) is drawn as a sphere. The halogen bond between the ligand (bromine atom, purple) and the backbone oxygen atom of Val239 is indicated by a dashed line (for details on the halogen bonding, see Figure 3). The orientation of the structure is according to Figure 1a.

Next, we elucidated the crystal structures of AtIspD in complex with **4a** (1.8 Å resolution, PDB code: 4NAK), **4b** (1.8 Å resolution, PDB code: 4NAL), and **4e** (1.8 Å resolution, PDB code: 4NAN), which resulted in well-defined electron-density maps for each of the bound ligands (Figures 2 and 4SI). Interestingly, binding of the compounds occurs in a cavity located in proximity to the active site and which is independent of the adjacent monomer. This pocket was already observed in studies with azolopyrimidine-type inhibitors **3a–c**.<sup>[10]</sup>

Nevertheless, the data presented here document a high degree of plasticity of this binding site, since the pseudilin derivatives differ in their molecular structure and mode of action compared to the azolopyrimidine ligands (Figure 5SI). With both pseudilin- and azolopyrimidine-type inhibitors there is a major conformational transition that affects predominantly amino acid residues Arg157 and Asp262. Notably, all the reported crystal structures of apo IspD lack this characteristic cavity.<sup>[19]</sup> In the apo as well as the holo



structures, Arg157 interacts with Asp262 and thereby keeps this ligand binding pocket locked. As shown in Figure 1c, binding of compound **4a** causes major structural rearrangements. Asp262 becomes solvent-exposed, and the interaction to Arg157 is abolished. Consequently, Arg157 moves into the CTP binding site, with the generation of specific hydrogen bonds with Asp179. This conformational twist prevents nucleotide binding by causing a clash with the ribose, and hence leads to enzyme inhibition. Thus, our results show that pseudilin derivatives act as allosteric inhibitors of IspD.

The crystal structures of *AtIspD* in complex with **4a** and **4b** reveal that the phenol and pyrrole rings of the ligands are in a *syn* conformation and are bound to a metal ion, which on the basis of the electron density and crystallization conditions we propose corresponds to cadmium(II). The metal ion is tetrahedrally coordinated to the phenolic hydroxy group and the pyrrole nitrogen atom of the inhibitors, the Gln238 side chain, and a water molecule with ion-to-ligand distances in the range of 2.2 to 3.7 Å (Figure 3). Besides this metal chelation, a bromine and a chlorine atom of the pseudilin derivatives (C-X) in the cocrystals of **4a** and **4b** appear perfectly poised for halogen bonding with the backbone carbonyl oxygen atom of the enzyme (Val239; O-Y, Figure 3).<sup>[20,21]</sup> This interaction is characterized by the requirement for nearly colinear alignment of the halogen-bond acceptor C-X with the halogen-bond donor atom at a distance less than the van der Waals distance, thus allowing the donor atom to orient its electron density into the  $\sigma$ -hole, which corresponds to the  $\sigma^*$ -orbital of the C-X bond. Typically, the distance between the halogen atom and the oxygen atom (X...O) is equal or less than the sum of their van der Waals radii (3.37 Å for Br...O, 3.27 Å for Cl...O),<sup>[21]</sup> while the angles are 165–180° for C-X...O and about 120° for X...O-Y.<sup>[21a,22]</sup> The X...O distance and the angles are 3.26 Å and 164°/112° for compound **4a** and 3.25 Å and 164°/111° for compound **4b**. The structural data thus illustrates that halogen bonding with the enzyme adds to the stabilization of the ligands through coordination with the metal ion, thereby enhancing their inhibitory effect. We next determined the crystal structure of *AtIspD* in complex with compound **4e**, which lacks a halogen

atom at the specific site in the *para*-position to the phenolic OH group. Interestingly, the X-ray data displayed that compound **4e** adopts two different conformations in the allosteric pocket of the enzyme, 70% *syn* and 30% *anti* (Figures 2b, 3c). In the latter conformation, the molecule is unable to chelate through the phenolic OH group to the Cd<sup>2+</sup> center, but forms a halogen bond between the *ortho*-bromine to the backbone oxygen of the protein (X...O distance and angles 3.17 Å and 170°/113°). Additional van der Waals interactions (C...C distances around 3.7 Å) between the protein and pseudilin ligands are found in the three complexes, in particular van der Waals contacts below 4 Å with the amino acid side chains of Gln238 and Val266, which intercalate the phenolic ring of the ligand.

As described in the literature, there are other possible targets for pseudilin-type inhibitors: 12- and 15-lipoxygenases, nonspecific liver esterase, and myosin ATPases.<sup>[23]</sup> Since pseudilin derivatives may have more than one cellular target, it seems likely that the overall effect of this class of natural products on organisms can be highly dependent on the species, as shown for example, by the altered IC<sub>50</sub> values between the IspD enzyme of the plant *A. thaliana* and the protozoan *P. vivax*. We consider the possibility that the IspD orthologues apart from *A. thaliana* either lack the allosteric pocket or this loop region does not show the same flexibility as seen in *AtIspD*, and we will address these questions by future mutational studies.

In conclusion, we demonstrate that halogenated marine alkaloids of the pseudilin-type bind into an allosteric pocket of *AtIspD*. They also inhibit *PvIspD* and are active against *P. falciparum* in cell-based assays. CTP binding by *AtIspD* is prevented by conformational changes, thereby locking the catalytic active site. However, it is still unknown whether there also exists a common regulation of the non-mevalonate pathway at the allosteric site of IspD through endogenous feedback mechanisms. This site is addressed by the pseudilin derivatives, which block the formation of the essential precursors IPP and DMAPP for terpene biosynthesis. Since halogenated marine natural products are abundant,<sup>[24]</sup> their halogen atoms should be further investigated in biostructural

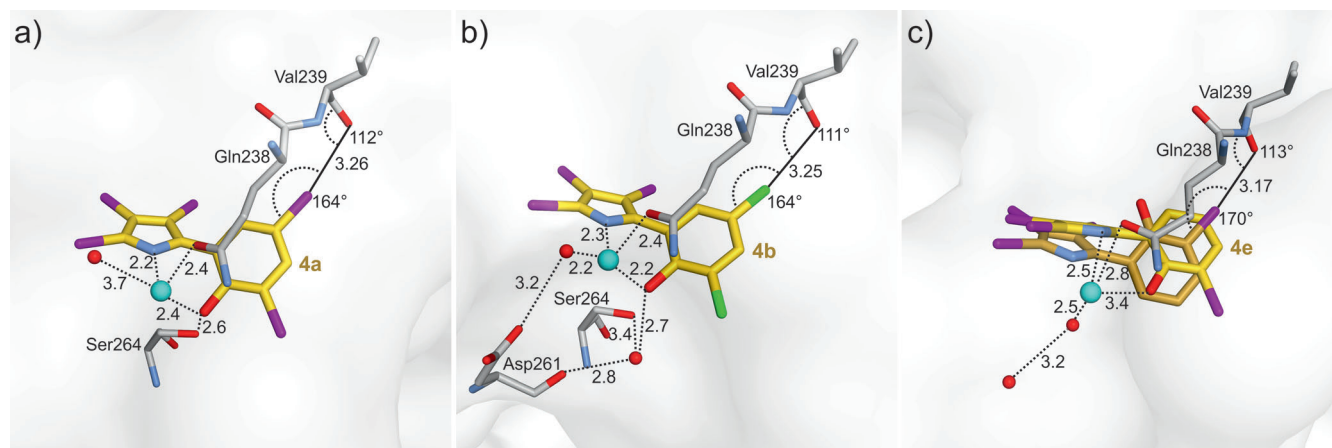


**Figure 3.** Halogen bonding and metal-ion interactions of compounds **4a**, **4b**, and **4e** (*syn* and *anti*) with *AtIspD*. Amino acid residues and compounds are presented as stick models, water molecules (red) and Cd<sup>2+</sup> ions (cyan) as spheres. Distances are given in Å.

studies on different targets for active participation in the molecular recognition processes such as halogen bonding.

Received: November 3, 2013

Revised: December 15, 2013

Published online: January 20, 2014

**Keywords:** allosteric inhibition · antiinfectives · drug discovery · halogen bonding · herbicides · pseudilins

- [1] a) Y. V. Ershov, *Appl. Biochem. Microbiol.* **2007**, *43*, 115–138; b) P. Gao, Y. Yang, C. Xiao, Y. Liu, M. Gan, Y. Guan, X. Hao, J. Meng, S. Zhou, X. Chen, J. Cui, *Eur. J. Pharmacol.* **2012**, *694*, 45–52; c) C. J. L. Murray, L. C. Rosenfeld, S. S. Lim, K. G. Andrews, K. J. Foreman, D. Haring, N. Fullman, M. Naghavi, R. Lozano, A. D. Lopez, *Lancet* **2012**, *379*, 413–431.
- [2] a) I. Abubakar, M. Zignol, D. Falzon, M. Raviglione, L. Ditiu, S. Masham, L. Adetifa, N. Ford, H. Cox, S. D. Lawn, B. J. Marais, T. D. McHugh, P. Mwaba, M. Bates, M. Lipman, L. Zijenah, S. Logan, R. McNeerney, A. Zumla, K. Sarda, P. Nahid, M. Hoelscher, M. Pletschette, Z. A. Memish, P. Kim, R. Hafner, S. Cole, G. B. Migliori, M. Maeurer, M. Schito, A. Zumla, *Lancet Infect. Dis.* **2013**, *13*, 529–539; b) A. Zumla, P. Nahid, S. T. Cole, *Nat. Rev. Drug Discovery* **2013**, *12*, 388–404.
- [3] M. Witschel, M. Rottmann, M. Kaiser, R. Brun, *PLoS Neglected Trop. Dis.* **2012**, *6*, e1805.
- [4] a) N. Qureshi, J. W. Porter in *Biosynthesis of Isoprenoid Compounds, Vol. 1* (Eds.: J. W. Porter, S. L. Spurgeon), Wiley, New York, **1981**; b) K. Bloch, *Steroids* **1992**, *57*, 378–383; c) T. J. Bach, *Lipids* **1995**, *30*, 191–202.
- [5] a) M. Rohmer, *Nat. Prod. Rep.* **1999**, *16*, 565–574; b) M. Rodriguez-Concepcion, A. Boronat, *Plant Physiol.* **2002**, *130*, 1079–1089; c) W. Eisenreich, A. Bacher, D. Arigoni, F. Rohdich, *Cell. Mol. Life Sci.* **2004**, *61*, 1401–1426; d) F. Rohdich, S. Lauw, J. Kaiser, R. Feicht, P. Köhler, A. Bacher, W. Eisenreich, *FEBS J.* **2006**, *273*, 4446–4458.
- [6] T. Masini, B. S. Kroezen, A. K. Hirsch, *Drug Discovery Today* **2013**, *18*, 1–7.
- [7] a) P. Mombelli, M. C. Witschel, A. W. van Zijl, J. G. Geist, M. Rottmann, C. Freymond, F. Röhl, M. Kaiser, V. Illarionova, M. Fischer, I. Siepe, W. B. Schweizer, R. Brun, F. Diederich, *ChemMedChem* **2012**, *7*, 151–158; b) N. Scherr, K. Röltgen, M. Witschel, G. Pluschke, *Antimicrob. Agents Chemother.* **2012**, *56*, 6410–6413.
- [8] Y. Matsue, H. Mizuno, T. Tomita, T. Asami, M. Nishiyama, T. Kuzuyama, *J. Antibiot.* **2010**, *63*, 583–588.
- [9] a) H. Jomaa, J. Wiesner, S. Sanderbrand, B. Altincicek, C. Weidemeyer, M. Hintz, I. Turbachova, M. Eberl, J. Zeidler, H. K. Lichtenthaler, D. Soldati, E. Beck, *Science* **1999**, *285*, 1573–1576; b) M. A. Missinou, S. Borrmann, A. Schindler, S. Issifou, A. A. Adegnika, P. B. Matsiegui, R. Binder, B. Lell, J. Wiesner, T. Baranek, H. Jomaa, P. G. Kremsner, *Lancet* **2002**, *360*, 1941–1942.
- [10] M. C. Witschel, H. W. Höffken, M. Seet, L. Parra, T. Mietzner, F. Thater, R. Niggeweg, F. Röhl, B. Illarionov, F. Rohdich, J. Kaiser, M. Fischer, A. Bacher, F. Diederich, *Angew. Chem.* **2011**, *123*, 8077–8081; *Angew. Chem. Int. Ed.* **2011**, *50*, 7931–7935.
- [11] a) P. R. Burkhold, R. M. Pfister, F. H. Leitz, *Appl. Microbiol.* **1966**, *14*, 649–653; b) R. J. Andersen, M. S. Wolfe, D. J. Faulkner, *Mar. Biol.* **1974**, *27*, 281–285.
- [12] V. Illarionova, J. Kaiser, E. Ostrozhenkova, A. Bacher, M. Fischer, W. Eisenreich, F. Rohdich, *J. Org. Chem.* **2006**, *71*, 8824–8834.
- [13] M. Witschel, F. Röhl, R. Niggeweg, T. Newton, *Pest Manage. Sci.* **2013**, *69*, 559–563.
- [14] a) H. Pudleiner, H. Laatsch, *Liebigs Ann. Chem.* **1990**, 423–432; b) D. R. Baker, J. G. Fenyves, J. J. Steffens, *ACS Symp. Ser.* **1992**, *504*, 1–7; c) H. Laatsch, B. Renneberg, U. Hanefeld, M. Kellner, H. Pudleiner, G. Hamprecht, H. P. Kraemer, H. Anke, *Chem. Pharm. Bull.* **1995**, *43*, 537–546.
- [15] a) R. Martin, A. Jäger, M. Böhl, S. Richter, R. Fedorov, D. J. Manstein, H. O. Gutzeit, H.-J. Knölker, *Angew. Chem.* **2009**, *121*, 8186–8190; *Angew. Chem. Int. Ed.* **2009**, *48*, 8042–8046; b) M. Preller, K. Chinthalapudi, R. Martin, H.-J. Knölker, D. J. Manstein, *J. Med. Chem.* **2011**, *54*, 3675–3685.
- [16] E. Yeh, J. L. DeRisi, *PLoS Biol.* **2011**, *9*, e1001138.
- [17] a) Since *P. falciparum* IspD cannot be expressed in an active form, PvIspD, the causative agent of malaria tertiana, was used. Both genes were codon-optimized; b) M. Fischer, unpublished results.
- [18] S. B. Richard, M. E. Bowman, W. Kwiatkowski, I. Kang, C. Chow, A. M. Lillo, D. E. Cane, J. P. Noel, *Nat. Struct. Biol.* **2001**, *8*, 641–648.
- [19] a) L. E. Kemp, C. S. Bond, W. N. Hunter, *Acta Crystallogr. Sect. D* **2003**, *59*, 607–610; b) J. Badger, J. M. Sauder, J. M. Adams, S. Antonysamy, K. Bain, M. G. Bergseid, S. G. Buchanan, M. D. Buchanan, Y. Batiyenko, J. A. Christopher, S. Emtage, A. Eroshkina, I. Feil, E. B. Furlong, K. S. Gajiwala, X. Gao, D. He, J. Hendle, A. Huber, K. Hoda, P. Kearins, C. Kissinger, B. Laubert, H. A. Lewis, J. Lin, K. Loomis, D. Lorimer, G. Louie, M. Maletic, C. D. Marsh, I. Miller, J. Molinari, H. J. Muller-Dieckmann, J. M. Newman, B. W. Noland, B. Pagarigan, F. Park, T. S. Peat, K. W. Post, S. Radojicic, A. Ramos, R. Romero, M. E. Rutter, W. E. Sanderson, K. D. Schwinn, J. Tresser, J. Winhoven, T. A. Wright, L. Wu, J. Xu, T. J. R. Harris, *Proteins Struct. Funct. Bioinf.* **2005**, *60*, 787–796; c) J. Behnen, H. Köster, G. Neudert, T. Craan, A. Heine, G. Klebe, *ChemMedChem* **2012**, *7*, 248–261; d) additional unpublished PDB codes: 2PX7, 3OKR, 4KT7.
- [20] a) O. Hassel, *Science* **1970**, *170*, 497–502; b) P. Politzer, P. Lane, M. C. Concha, Y. Ma, J. S. Murray, *J. Mol. Model.* **2007**, *13*, 305–311; c) T. Clark, M. Hennemann, J. S. Murray, P. Politzer, *J. Mol. Model.* **2007**, *13*, 291–296; d) P. Metrangolo, F. Meyer, T. Pilati, G. Resnati, G. Terraneo, *Angew. Chem.* **2008**, *120*, 6206–6220; *Angew. Chem. Int. Ed.* **2008**, *47*, 6114–6127; e) J. S. Murray, P. Lane, P. Politzer, *J. Mol. Model.* **2009**, *15*, 723–729; f) Y. Lu, Y. Wang, W. Zhu, *Phys. Chem. Chem. Phys.* **2010**, *12*, 4543–4551; g) T. M. Beale, M. G. Chudzinski, M. G. Sarwar, M. S. Taylor, *Chem. Soc. Rev.* **2013**, *42*, 1667–1680.
- [21] a) P. Auffinger, F. A. Hays, E. Westhof, P. S. Ho, *Proc. Natl. Acad. Sci. USA* **2004**, *101*, 16789–16794; b) Y. Lu, T. Shi, Y. Wang, H. Yang, X. Yan, X. Luo, H. Jiang, W. Zhu, *J. Med. Chem.* **2009**, *52*, 2854–2862; c) L. A. Hardegger, B. Kuhn, B. Spinnler, L. Anselm, R. Ecabert, M. Stihle, B. Gsell, R. Thoma, J. Diez, J. Benz, J.-M. Plancher, G. Hartmann, D. W. Banner, W. Haap, F. Diederich, *Angew. Chem.* **2011**, *123*, 329–334; *Angew. Chem. Int. Ed.* **2011**, *50*, 314–318; d) L. A. Hardegger, B. Kuhn, B. Spinnler, L. Anselm, R. Ecabert, M. Stihle, B. Gsell, R. Thoma, J. Diez, J. Benz, J.-M. Plancher, G. Hartmann, Y. Isshiki, K. Morikami, N. Shimma, W. Haap, D. W. Banner, F. Diederich, *ChemMedChem* **2011**, *6*, 2048–2054.
- [22] A. Bondi, *J. Phys. Chem.* **1964**, *68*, 441–451.
- [23] B. Zhang, K. M. Watts, D. Hodge, L. M. Kemp, D. A. Hunstad, L. M. Hicks, A. R. Odoms, *Biochemistry* **2011**, *50*, 3570–3577.
- [24] a) M. T. Cabrita, C. Vale, A. P. Rauter, *Mar. Drugs* **2010**, *8*, 2301–2317; b) T. S. Elliott, A. Slowey, Y. Ye, S. J. Conway, *MedChemComm* **2012**, *3*, 735–751; c) G. W. Gribble, *The Alkaloids, Vol. 71*, Academic Press, Oxford, **2012**.
- [25] P. Kuzmič, *Anal. Biochem.* **1996**, *237*, 260–273.